Generation of highly-retrievable atom–photon entanglement with a millisecond lifetime via a spatially-multiplexed cavity

Hai Wang (wanghai@sxu.edu.cn)
Shanxi University https://orcid.org/0000-0002-8952-3734
Minjie Wang
Shanxi University
Shengzhi wang
Tengfei Ma
ya li
yan xie
haole jiao
hailong liu
Shujing Li

Article

Keywords:

Posted Date: June 22nd, 2022

DOI: https://doi.org/10.21203/rs.3.rs-1738478/v1

Generation of highly-retrievable atom–photon entanglement with a millisecond lifetime via a spatially-multiplexed cavity

Minjie Wang, Shengzhi Wang, Tengfei Ma, Ya Li, Yan Xie, Haole Jiao, Hailong Liu, Shujing Li, Hai Wang*

The State Key Laboratory of Quantum Optics and Quantum Optics Devices, Institute of Opto-Electronics, Shanxi University, Taiyuan 030006

China Collaborative Innovation Center of Extreme Optics, Shanxi University, Taiyuan 030006, China

Qubit memory that is entangled with photonic qubit is the building block for quantum repeaters. Realizing ensemble-based repeaters requires qubit simultaneously featuring high retrieval efficiencies and long lifetimes. So far, the longest memory time at 50% retrieval efficiency for entanglement storage reaches ~40 μs. Here, by coupling cold atoms to two spatially-distinctive modes of a polarization-interferometer-based cavity, we achieve cavity-perfectly-enhanced and long-lived atom-photon entanglement. A write-laser beam is applied onto cold atoms, we then create a magnetic-field-insensitive spin-wave qubit that is entangled with the photonic qubit encoded onto two arms of the interferometer. By applying a read beam, the spin-wave qubit is converted to a photonic qubit,

whose two modes are resonant with the cavity. Our experimental data shows that zero-delay intrinsic retrieval efficiency is up to 77% and 1/e lifetime 1ms. At 50% efficiency, the storage time reaches $540\mu s$, which is 13.5 times longer than the best reported result.

Introduction. — A qubit memory entangled with a photonic qubit forms the building block (repeater node) for long-distance quantum communications [1-3], large-scale quantum internet [4, 5], and quantum clock network [6] through a quantum repeater (QR) [1, 2]. In past decades, optical quantum memories (QMs) have been experimentally demonstrated with various matter systems [7] such as atomic ensembles [1, 8] and single-quantum systems including individual atoms [9, 10], ions [11], and solid-state spins [12, 13]. Compared with the QMs in a single-quantum system, the atomic-ensemble-based QMs feature collective enhancement and promise higher retrieval efficiencies [1].With atomic ensembles, optical QMs has been demonstrated via various schemes [7, 8, 14, 15] including Duan–Lukin–Cirac–Zoller (DLCZ) protocol [1, 16-38] and "read-write" [14] (or called "absorptive" [15]) schemes such as electromagnetically-induced-transparency (EIT) dynamics [39-52], photon echoes [53-60], Raman memory [61-63] and its variants [64, 65], etc. In contrast to the "read-write" schemes, the DLCZ protocol establishes QMs via spontaneous Raman emissions of Stokes photon induced by a write pulse instead of storing single specific (incoming) photons [14]. Since DLCZ protocol can directly produces non-classically correlated [16-28] or entangled [29-38] pairs of a Stokes photon and a spin-wave memory, it benefits for practically realizing QRs [1].

High-efficiency and long-lived QMs are required for effectively

achieving quantum information tasks [3, 7]. In long-distance entanglement distribution through QRs, a 1% increase in retrieval efficiency can improve the repeater rate by 10–14% [1]. The lifetime at 50% efficiency is defined as a benchmark of memory nodes in QRs [3]. Additionally, establishing entanglement between two nodes separated by L=300 km in a ‘‘heralded’’ fashion requires storing a qubit for at least L/c=1.5 ms [34, 66], with c being the speed of light in fibers. To realize long-lived QMs, significant progresses have been made with cold atomic ensembles [19-24, 32-34, 56]. These studies show that atomic-motion-induced decoherence can be suppressed either by lengthening spin-wave wavelengths [20, 21, 32, 34，55] or confining the atoms in optical lattices [22-24, 32-33]. Inhomogeneous-broadening-induced decoherence may be suppressed by storing SWs in magnetic-field-insensitive (MFI) coherences, which includes three spin transitions $|5S_{1/2}, F=1, m_F=\pm 1,0\rangle \leftrightarrow |5S_{1/2}, F=2, m_F=\pm 1,0\rangle$ for ^{87}Rb atoms, where, $m_{F_1}=0 \leftrightarrow m_{F_2}=0$ is called clock coherence. In a specific DLCZ experiment, one can store spin waves (SWs) in one of the MFI coherences [24].

In previous long-lived atom–photon entanglement generation via DLCZ protocol [32], a Mach–Zehnder interferometer, whose two arms are used to encode photonic qubit, is built around optical-lattice Rb atoms. Two spatially-distinctive SWs associated with the clock coherence and correlated with the Stokes fields emitting into the two arms, respectively,

are created by a write beam and stored as memory qubit. To maintain maximal entanglement, the relative phase between the two arms was actively stabilized by coupling an auxiliary laser beam into the interferometer. The lifetime of entanglement storage reaches 0.1 s but the retrieval efficiency is only ~16% due to weak atom-photon interactions [32]. The high-efficiency memories for single photons have been achieved by using either high-optical-depth cold atoms [50, 51] or coupling moderate-optical-depth atoms with a low-finesse optical cavity [21, 24, 30, 33]. In high-optical-depth cold atoms, the efficiencies of the storages of single-photon entanglement [51] and polarization qubit [50] reach ~85%, while their lifetimes are only ~15 μs. Using the cavity-enhanced scheme, Pan's group demonstrated intrinsic retrieval efficiency up to ~76% in a DLCZ experiment that create polarization atom-photon entanglement [30]. In that experiment, the spin-wave qubit is stored as superimposition of magnetic-field-sensitive and MFI coherences. Limiting to fast decoherence of the magnetic-field-sensitive coherence, the memory lifetime is only ~30 μs [30]. Efficient and long-lived atom-photon quantum correlations has been demonstrated by applying a write beam onto optical-lattice atoms, where the atomic SW is stored in the clock coherence and coupled to a ring cavity with its length being locked [24]. The efficiencies at zero delay reach to 76% and at 50-ms storage time to 50%. [24]. On this basis, Pan's group demonstrated cavity-enhanced atom-photon entanglement with sub-second

lifetime [33]. To create H- and V- polarized Stokes emissions used for encoding photonic qubit, the group applied two write beams onto the lattice atoms. The two SW modes, both associated with the clock coherence and correlated with the H- and V- polarized Stokes fields, respectively, are stored as memory qubit. That experiment [33] removes the M–Z interferometer used in Ref. [32] and then avoids experimental complexity due to interferometer-mediated coupling between atoms and a cavity. However, that experiment require dual read-laser beams to retrieve the two SWs, which leads to cross retrievals and decrease qubit retrieval efficiency by one quarter compared to that of a single-mode SW at all storage times [33]. Due to the imperfect readout, the efficiency of retrieving the spin-wave qubit was only ~58% at zero delay [33], about three quarters that of the single-mode one (~76%) [24]. At 50% efficiency, the storage time was only ~40 μs. So far, entanglement storage that has high-efficiency and long-lived performances simultaneously remains a challenge. Here, we overcome the imperfect retrieval in Ref.[33] by coupling cold atoms to a two-mode ring cavity based on a polarization interferometer. The interferometer is mainly formed by two beam displacers (BD1 and BD2). The relative phase between the two arms is passively stabilized, which has been demonstrated in previous experiments [43, 49-51, 67-68]. Two optical lenses are inserted in the interferometer, which make interferometer's two arms (A_R and A_L) crossway pass-through

cold atoms. By arranging interferometer's configuration, the ring cavity simultaneously supports the two arms as cavity modes cf. below. By applying a write beam, we create two SWs associated with the clock coherence and correlated with the Stokes emissions into the cavity modes A_R and A_L, respectively. The two SWs are retrieved by a read beam and then avoids the cross retrieval. The two Stokes (retrieved) fields forms a photonic qubit and resonate with the cavity. The intrinsic qubit retrieval efficiencies reach 50% (66.7%) at 540-μs (230-μs) storage time, which is 13.5 (24) times higher than the best reported results [33] ([30]). The measured Bell parameter for atom-photon entanglement is 2.5 ± 0.02 at zero delay. Unlike the previous experiments [21, 24, 30, 33, 69-70], our experiment demonstrated that the two arms of the polarization interferometer can be simultaneously supported by a ring cavity, which enable perfect retrieval in cavity-enhanced and long-lived atom–photon entanglement.

As shown in the schematic diagram Fig.1a, the heart of experimental setup is a ring cavity inserted by a polarization interferometer with cold atoms (circled by dashed line). The ring cavity is formed by three flat mirrors ($HR_{1,2,3}$) with high reflection and a flat output coupler (OC) with a reflectance of 80%. It supports TEM_{00} mode A_{00} that propagates in the whole cavity [71]. When the polarization interferometer is inserted in the cavity, the A_{00} mode has the path from BD2 to BD1 via OC and HR_1 (black

line in Fig.1a). When the mode A_{00} propagates along clockwise, it will be split into H (horizontally) and V (vertically) -polarized components by BD2, both direct into the interferometer's two arms A_L and A_R, respectively. Two optical lenses lens1 and lens2, which have the same focus length F_0, are inserted in the interferometer. Then, the arms A_L and A_R crossway pass through the atoms and couple with the atoms, respectively. The more detailed explanations of the A_L and A_R paths can be found in Supplementary material [71]. By setting the distance between lens1 and lens2 to be $2F_0$, the two arms are well recombined into the mode A_{00} by BD1 and then supported by the cavity. In our experiment, the spot size of A_{00} is set to be a large value (5.2mm) in order to decrease the mode losses escaping from the cavity. The measured loss of the mode A_{00} via A_R (A_L) path escaping from cavity per round trip is ~3.2% (3.2%). So, the two arms A_R and A_L may serve as cavity modes.

The atomic ground levels $|a\rangle=|5S_{1/2},F=1\rangle$ and $|b\rangle=|5S_{1/2},F=2\rangle$ together with the excited level $|e_1\rangle=|5P_{1/2},F'=1\rangle$ ($|e_2\rangle=|5P_{1/2},F'=2\rangle$) form a Λ -type system [Fig.1b and c]. After the atoms are prepared in the Zeeman state $|a,m_{F_a}=0\rangle$, we start spin-wave-photon (atom-photon) entanglement generation. At the beginning of a trial [71], a 795-nm σ^+ -polarized write pulse with red-detuned by 110 MHz to the $|a\rangle\rightarrow|e_1\rangle$ transition is applied to the atoms along z-axis through a beam splitter BS1. This write pulse induces the Raman transition $|a,m_{Fa}=0\rangle\rightarrow|b,m_{Fb}=0\rangle$ via $|e_1,m_{Fe}=1\rangle$ [Fig. 1b],

which emit σ^+-polarized Stokes photons and simultaneously create SW excitations associated with the clock coherence $|m_a=0\rangle \leftrightarrow |m_b=0\rangle$. If the Stokes photon is emitted into the cavity mode A_R (A_L) and moves towards the right, one collective excitation will be created in the SW mode M_R (M_L) defined by the wave-vector $k_{M_R}=k_W-k_{S_R}$ ($k_{M_L}=k_W-k_{S_L}$), where k_W is the wave-vector of the write pulse and k_{S_R} (k_{S_L}) that of the Stokes photon in the cavity A_R (A_L) mode. The angle between the mode A_R (A_L) and the write beam is $\theta_R \approx 0.053^0$ ($\theta_A \approx -0.053^0$) [71]. Such small angles make SW wavelengths be long, suppressing atomic-motion-induced decoherence [34]. The σ^+-polarized Stokes fields in A_R and A_L modes propagate along clockwise, which are transformed into *H*-polarized fields by a λ/4 wave-plate QW_S. Furthermore, the *H*-polarized field in A_L is transformed into *V*-polarized field by a λ/2 wave-plate HW_S. Both fields are combined into the cavity mode A_{00} by BD2 and form a Stokes qubit S_{qbit}. As shown in Fig. 1(b), the write pulse also induces the Raman transition $|a,m_{Fa}=0\rangle \rightarrow |b,m_{Fb}=2\rangle$ via $|e_1,m_{Fe}=1\rangle$, which emit σ^--polarized Stokes photons and simultaneously create SWs associated with the magnetic-field-sensitive coherence $|m_{Fa}=0\rangle \leftrightarrow |m_{Fb}=2\rangle$. If the σ^--polarized Stokes photon direct into the mode A_R (A_L) and propagate along clockwise, it will be transformed into *V*- (*H*-) polarized photon by the QW_S (QW_S and HW_S) and then is excluded from the A_{00} cavity mode by BD2. Propagating in A_{00}, the S_{qbit}

returns the interferometer. It is split into H and V -polarized fields by BD1, which direct into A_R and A_L modes, respectively. Both Stokes modes are transformed into σ^+ -polarization by wave-plates [71] and then interact with the atoms again. The spin-wave qubit formed by M_R and M_L modes is entangled with S_{qbit}, which is written as:

$$\Phi_{a\text{-}p} = \left(|H\rangle_S |M_R\rangle + e^{i\varphi_S} |V\rangle_S |M_L\rangle\right)/\sqrt{2} \quad (1)$$

where, $|H\rangle_S$ ($|V\rangle_S$) denotes the H- (V-) polarized Stokes photon, $|M_R\rangle$ ($|M_L\rangle$) one SW excitation in the mode M_R (M_L), φ_S the relative phase between the two Stokes emissions from the atoms to BD2 via A_R and A_L paths.

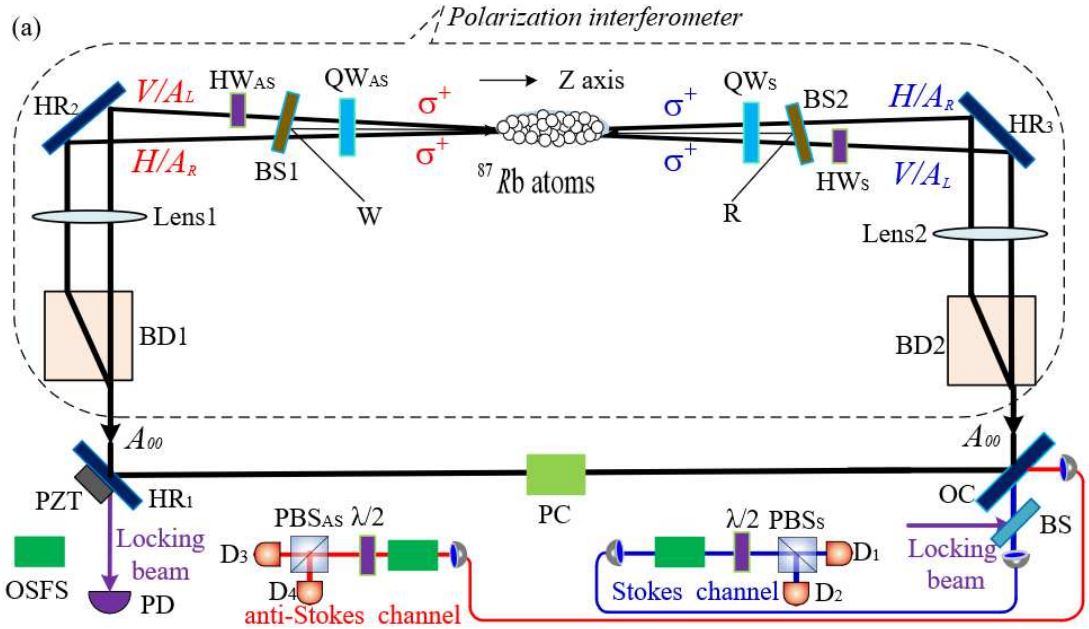

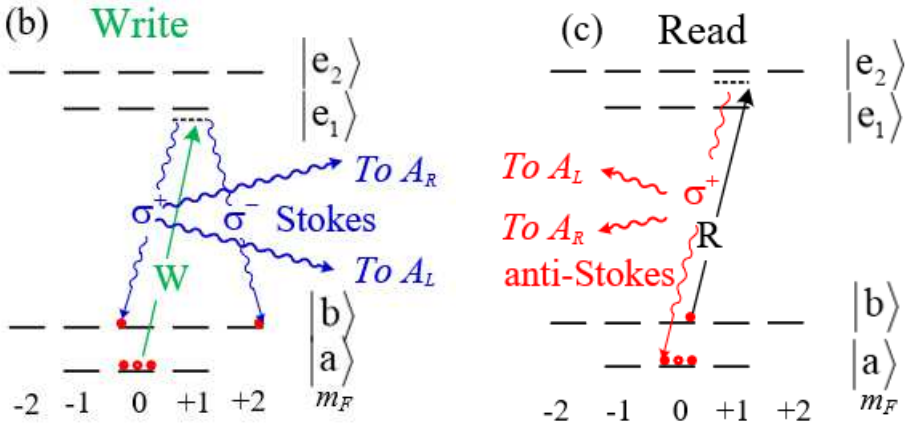

Fig. 1. Schematic diagram for experimental setup (a): A polarization interferometer formed by two beam displacers (BD1 and BD2) is inserted into a ring cavity. A locking laser pulse is coupled to the A_{00} mode through a beam splitter (BS). Leaks of the cavity-locking pulse from HR_3 are detected by a fast photodiode (PD) to generate error signals. The error signals are amplified and used to drive a piezoelectric transducer (PZT) to stabilize the cavity length. OSFS: optical-spectrum-filter set [34]; PC: phase compensator; BS1 (BS2): non-polarizing beam splitter with a reflectance of 1% (3%). (b) and (c) are relevant atomic levels involved in the write and read processes, respectively, W (R): write (read) laser.

After a storage time t, we apply a σ^+-polarized read pulse onto the atoms through a beam splitter BS2. The read pulse is red-detuned by 110 MHz to the $|b\rangle \rightarrow |e_2\rangle$ transition and counter-propagates with the write beam, which convert the spin-wave $|M_R\rangle$ ($|M_L\rangle$) into anti-Stokes photon. The anti-Stokes photon retrieved from $|M_R\rangle$ ($|M_L\rangle$) is σ^+-polarized and emitted into the spatial mode determined by the wave-vector constraint $k_{AS_R} \approx -k_{S_R}$ ($k_{AS_L} \approx -k_{S_L}$), i.e., it propagates along anti-clockwise in the arm A_R

(A_L). The anti-Stokes fields in A_R and A_L are transformed into *H*-polarized fields by a λ/4-plate QW_{AS}. Furthermore, the anti-Stokes field in A_L is transformed into *V*-polarized field by a λ/2-plate HW_{AS}. Both fields are combined into an anti-Stokes qubit AS_{qbit} by BD1 and then propagate in A_{00} mode along anti-clockwise. The AS_{qbit} is split into *H*- and *V*-polarized fields by BD2, which direct into A_R and A_L modes, respectively. Next, both anti-Stokes modes are transformed into σ^+ -polarization by wave-plates [71] and then interact with the atoms. So, the atoms are repeatedly coupled with the cavity modes. The two-photon entangled state is written as:

$$\Phi_{\text{p-p}} = \left(|H\rangle_S |H\rangle_{AS} + e^{i(\varphi_S + \varphi_{AS})} |V\rangle_S |V\rangle_{AS}\right) / \sqrt{2} \qquad (2).$$

where, the subscript *S* (*AS*) denotes the Stokes (anti-Stokes) photon, φ_{AS} the relative phase between the two anti-Stokes emissions from the atoms to BD1 via A_R and A_L paths. In our experiment, the sum of φ_S and φ_{AS} is passively set to zero with a phase compensator [71]. The cavity length is actively stabilized by coupling a cavity-locking beam through OC. The Stokes and anti-Stokes fields are tuned to resonate with the ring cavity [71]. As shown in Fig.1, the escaped Stokes (anti-Stokes) photon from OC is coupled to a sing-mode fiber and then is guided into a polarization-beam splitter PBS_S (PBS_{AS}). Two outputs of PBS_S (PBS_{AS}) are sent to single-photon detectors D_1 (D_3) and D_2 (D_4). The polarization angle θ_S (θ_{AS}) of the Stokes (anti-Stokes) field is changed by rotating a λ/2-plate

before PBS_S (PBS_{AS}).

The intrinsic retrieval efficiency of the SW qubit can be measured as $R_{qbit}^{inc} = P_{S,AS} / (\eta_{TD} P_S)$, where $P_{S,AS} = P_{D_1,D_3} + P_{D_2,D_4}$; P_{D_1,D_3} (P_{D_2,D_4}) is the probability of detecting a coincidence between the detectors D_1 (D_2) and D_3 (D_4) for $\theta_S = \theta_{AS} = 0°$, $P_S = P_{D_1} + P_{D_2}$, where P_{D_1} (P_{D_2}) is the probability of detecting a Stokes photon at D_1 (D_2); $\eta_{TD} = \eta_{esp}\eta_t\eta_D$ is the total detection efficiency of the read-out (anti-Stokes) channel, which includes the efficiency of light escaping from the ring cavity, $\eta_{esp} \approx 60\%$, the transmission efficiency from the cavity to the detectors, $\eta_t \approx 36\%$ [71], and the detection efficiency of the single-photon detectors, $\eta_D \approx 68\%$. Thus, the total detection efficiency is $\eta_{TD} \approx 15\%$. Moreover, the intrinsic retrieval efficiency for an individual SW M_L (M_R) mode is defined as $R_L^{inc} = P_{D_1,D_3} / (\eta_{TD} P_{D_1})$ ($R_R^{inc} = P_{D_2,D_4} / (\eta_{TD} P_{D_2})$). Fig.2 plots the measured efficiencies R_{qbit}^{inc} (red circle dots), R_L^{inc} (blue square dots), and R_R^{inc} (green triangle dots) as functions of storage time *t*. From the figure, we see that $R_{qbit}^{inc} \approx R_L^{inc} \approx R_R^{inc}$ for different times *t,* which means that the retrieval efficiency for an SW qubit is the same as that for a single-mode SW. This shows that the efficiency loss of retrieving the qubit, which is a key limit in state-of-the-art work [33], is overcome in our experiment. The solid grey curve is the fit to the retrieval efficiencies R_{qbit}^{inc}, R_L^{inc}, and R_R^{inc} according to the function $R(t) = R_0 \left(\exp\left(-t^2/\tau_0^2\right) + \exp\left(-t/\tau_0\right)\right)/2$, which yields retrieval efficiencies $R_0 = 77\%$, $R(t = 0.23\mathrm{ms}) \approx 66.7\%$ and $R(t = 0.54\mathrm{ms}) \approx 50\%$, together with a memory lifetime $\tau_0 \approx 1ms$.

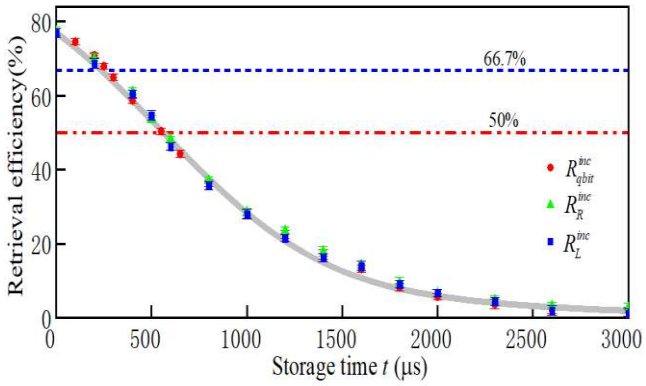

Fig.2 Intrinsic retrieval efficiencies as a function of storage time t for $\chi = 1\%$. Error bars represents 1 standard deviation.

Next, we measure the Clauser–Horne–Shimony–Holt (CHSH) inequality, which is a type of Bell inequality, to confirm the spin-wave-photon entanglement state $\Phi_{a\text{-}p}$. The Bell CHSH parameter is defined as $S_{Bell} = \left|E(\theta_S,\theta_{AS}) - E(\theta_S,\theta'_{AS}) + E(\theta'_S,\theta_{AS}) + E(\theta'_S,\theta'_{AS})\right| < 2$ with the correlation function $E(\theta_S,\theta_{AS})$, which is written as $\frac{C_{13}(\theta_S,\theta_{AS}) + C_{24}(\theta_S,\theta_{AS}) - C_{14}(\theta_S,\theta_{AS}) - C_{23}(\theta_S,\theta_{AS})}{C_{13}(\theta_S,\theta_{AS}) + C_{24}(\theta_S,\theta_{AS}) + C_{14}(\theta_S,\theta_{AS}) + C_{23}(\theta_S,\theta_{AS})}$. For example, $C_{13}(\theta_S,\theta_{AS})$ ($C_{24}(\theta_S,\theta_{AS})$) denotes the coincidence counts between the detectors D_1 (D_2) and D_3 (D_4) for the polarization angles θ_S and θ_{AS}. We used the canonical settings $\theta_S = 0°$, $\theta'_S = 45°$, $\theta_{AS} = 22.5°$, and $\theta'_{AS} = 67.5°$ in measuring the Bell parameter S_{Bell}. Fig. 3 shows the decay of S_{Bell} as a function of storage time t (blue squares) for $\chi = 2\%$. At $t \approx 0\ \mu s$, $S_{Bell} = 2.5 \pm 0.02$, while at t =1.15 ms, $S_{Bell} = 2.05 \pm 0.03$. These violate the Bell inequality by 25 and 1.7 standard deviations, respectively. Furthermore, at t=2.6 ms, $S_{Bell} = 1.15 \pm 0.03$, which corresponds to a fidelity of $F \approx 0.55$ and exceeds the bound of 0.5 required to observe entanglement for a Bell state.

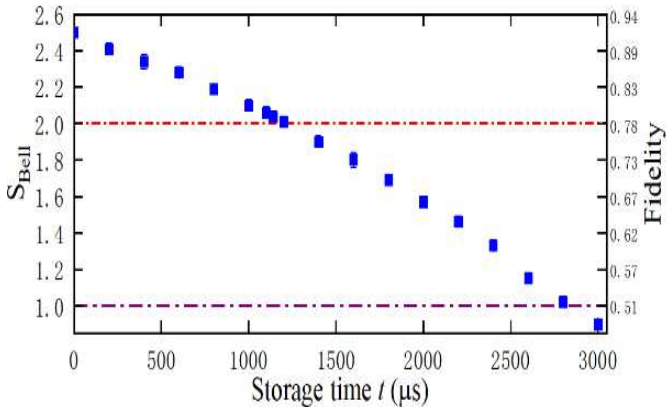

Fig. 3. Measured Bell parameter as a function of storage time t for $\chi = 2\%$. Error bars represent 1 standard deviation.

For comparison, we plot Fig. 4 to show the measured retrieval efficiencies for the memories restricted to qubit storages as functions of storage times in various systems via different schemes. One can see that our experimental result of 50% (66.7%) intrinsic retrieval efficiency for a storage time of 540 μs (230 μs) is 13.5 (24) times higher than the previously reported best result [33] ([30]).

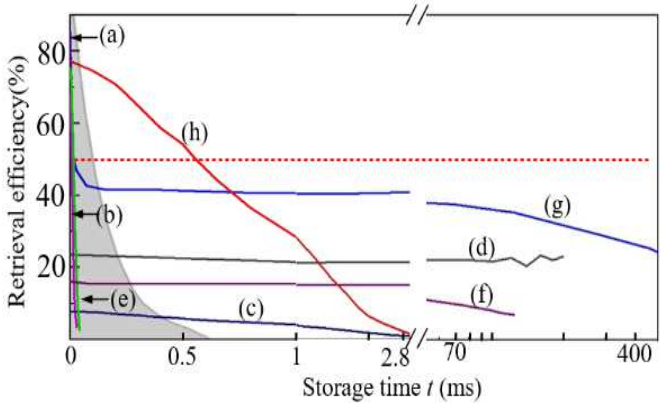

Fig. 4. Retrieval efficiencies of memory qubit vs storage time t in various systems. The shaded region shows the result for an ideal-optical-fiber loop. Curves (a) and (b) are the results for storages of single-photon [50] and weak-coherent-light [49] qubits via EIT in high-optical-density cold atoms. Curve (c) represents the results for qubit

memory stored as MFI spin waves via EIT in cold atoms [44]. Curve (d) represents single-photon qubit storage via EIT in single atoms [10]. Curves (e), (f), (g) and (h), corresponding to the results in Refs. [30], [32], [33] and our experiment, respectively, represent qubit memories via DLCZ protocol.

Conclusion. **—**The use of the polarization interferometer in the cavity enables us to apply a write beam to create two SW modes of the memory qubit, both associated with the clock coherence and coupled to the ring cavity. Thanks to phase-matching condition, the two SW modes are retrieved by a read beam, which avoids the cross retrievals in Ref. [33]. The relative phase between the two arms is passively stabilized and easily set to be zero by the phase compensator. On this basis, we achieve quadruple resonance of the cavity with the Stokes and retrieved fields propagating in the cavity modes A_R and A_L, respectively. This represents the first demonstration of an atomic ensemble simultaneously coupled into two TEM_{00} modes of a cavity. We thus achieve atom-photon entanglement with highly-retrievable efficiency (77%) and millisecond lifetime. By selecting more cavity modes to couple with the atoms, we will achieve massively-multiplexed and high-reversible spin-wave–photon entanglement with long lifetime and then is used for achieving long-distance (1000-km) entanglement distributions through QR [71].

In this experiment, we suppress inhomogeneous-broadening-induced

decoherence by storing both SWs in the clock coherence. Atomic-motion-induced dephasing is suppressed by using the storage scheme of the long-wavelength SW [34]. The lifetime in our presented experiment is ~1 ms, which can be extended to hundreds of milliseconds by loading the cold atoms into optical lattices and using magic field values [33].

DATA AVAILABILITY

The data that support the findings of this study are available from the authors upon request.

ACKNOWLEDGEMENTS

We acknowledge funding support from Key Project of the Ministry of Science and Technology of China (Grant No. 2016YFA0301402); The National Natural Science Foundation of China (Grants: No. 11475109, No. 11974228), Fund for Shanxi "1331 Project" Key Subjects Construction.

AUTHOR CONTRIBUTIONS

H.W. conceived the research. H.W., S.-J.L. and M.-J.W. designed the experiment. M.-J. W., S.-Z.W., T.-F.M. setup the experiment with assistances from all other authors. M.-J.W. took the data. M.-J.W. analyzed the data. H.W. wrote the paper.

Competing interests: The authors declare no competing interests.

*Corresponding author: wanghai@sxu.edu.cn

References:

[1] N. Sangouard, C. Simon, H. de Riedmatten, N. Gisin, Quantum repeaters based on atomic ensembles and linear optics. Rev. Mod. Phys. **83**, 33-80 (2011).

[2] L. -M. Duan, M. D. Lukin, J. I. Cirac, a. P. Zoller, Long-distance quantum communication with atomic ensembles and linear optics. Nature **414**, 413-418 (2001).

[3] C. Simon, Towards a global quantum network. Nat. Photon. **11**, 678-680 (2017).

[4] H. J. Kimble, The quantum internet. Nature **453**, 1023-1030 (2008).

[5] S. Wehner, D. Elkouss, R. Hanson, Quantum internet: A vision for the road ahead. **Science** 362, 303 (2018).

[6] P. Kómár, E. M. Kessler, M. Bishof, L. Jiang, A. S. Sørensen, J. Ye, and M. D. Lukin, A quantum network of clocks. Nat. Phys. **10**, 582 (2014)

[7] F. Bussières, N. Sangouard, M. Afzelius, H. de Riedmatten, C. Simon, and W. Tittel, Prospective applications of optical quantum memories. Journal of Modern Optics **60**, 1519 (2013).

[8] A. I. Lvovsky, B. C. Sanders, W. Tittel, Optical quantum memory. Nat. Photon. **3**, 706-714 (2009).

[9] T. van Leent, M. Bock, R. Garthoff, K. Redeker, W. Zhang, T. Bauer, W. Rosenfeld, C. Becher, H. Weinfurter, Long-Distance Distribution of Atom-Photon Entanglement at Telecom Wavelength. Phys. Rev. Lett. **124**, 010510 (2020).

[10] M. Körber, O. Morin, S. Langenfeld, A. Neuzner, S. Ritter, G. Rempe, Decoherence-protected memory for a single-photon qubit. Nat. Photon. **12**, 18-21 (2017).

[11] B.B. Blinov, D.L. Moehring, L.-M Duan, C. Monroe, Observation of entanglement between a single trapped atom and a single photon. Nature **428**, 153-157 (2004).

[12] B. Hensen, H. Bernien, A. E. Dreau, A. Reiserer, N. Kalb, M. S. Blok, J. Ruitenberg, R. F. Vermeulen, R. N. Schouten, C. Abellan, W. Amaya, V. Pruneri, M. W. Mitchell, M. Markham, D. J. Twitchen, D. Elkouss, S. Wehner, T. H. Taminiau, R. Hanson, Loophole-free Bell inequality violation using electron spins separated by 1.3 kilometres. Nature **526**, 682-686 (2015).

[13] A. Delteil, Z. Sun, W.-b. Gao, E. Togan, S. Faelt, A. Imamoğlu, Generation of heralded entanglement between distant hole spins. Nat. Phys. **12**, 218-223 (2015).

[14] Mikael Afzelius, Nicolas Gisin, and Hugues de Riedmatten, Quantum memory for photons, Physics Today **68**, 12, 42 (2015).

[15] K. Heshami, D. G. England, P. C. Humphreys, P. J. Bustard, V. M.

Acosta, J. Nunn, B. J. Sussman, Quantum memories: emerging applications and recent advances. Journal of Modern Optics **63**, 2005-2028 (2016).

[16] A. Kuzmich, W. P. Bowen, A. D. Boozer, A. Boca, C. -W. Chou, L.-M. Duan, a. H. J. Kimble, Generation of nonclassical photon pairs for scalable quantum communication with atomic ensembles. Nature **423**, 731-734 (2003).

[17] Julien Laurat, Hugues de Riedmatten, Daniel Felinto, Chin-Wen Chou, E. W., Schomburg, and H. Jeff Kimble. Efficient retrieval of a single excitation stored in an atomic ensemble. Opt. Express **14**, 6912-6918 (2006).

[18] J. Simon, H. Tanji, J. K. Thompson, V. Vuletic, Interfacing collective atomic excitations and single photons. Phys. Rev. Lett. **98**, 183601 (2007).

[19] D. Felinto, C. W. Chou, H. de Riedmatten, S. V. Polyakov, H. J. Kimble, Control of decoherence in the generation of photon pairs from atomic ensembles. Phys. Rev. A **72**, 053809 (2005).

[20] B. Zhao, Y.-A. Chen, X.-H. Bao, T. Strassel, C.-S. Chuu, X.-M. Jin, J. Schmiedmayer, Z.-S. Yuan, S. Chen, J.-W. Pan, A millisecond quantum memory for scalable quantum networks. Nat. Phys. **5**, 95-99 (2008).

[21] X.-H. Bao, A. Reingruber, P. Dietrich, J. Rui, A. Dück, T. Strassel, L. Li, N.-L. Liu, B. Zhao, J.-W. Pan, Efficient and long-lived quantum memory with cold atoms inside a ring cavity. Nat. Phys. **8**, 517-521 (2012).

[22] R. Zhao, Y. O. Dudin, S. D. Jenkins, C. J. Campbell, D. N. Matsukevich, T. A. B. Kennedy, A. Kuzmich, Long-lived quantum memory. Nat. Phys. **5**, 100-104 (2008).

[23] A. G. Radnaev, Y. O. Dudin, R. Zhao, H. H. Jen, S. D. Jenkins, A. Kuzmich, T. A. B. Kennedy, A quantum memory with telecom-wavelength conversion. Nat. Phys. **6**, 894-899 (2010).

[24] S.-J. Yang, X.-J. Wang, X.-H. Bao, J.-W. Pan, An efficient quantum light–matter interface with sub-second lifetime. Nat. Photon. **10**, 381-384 (2016).

[25] E. Bimbard, R. Boddeda, N. Vitrant, A. Grankin, V. Parigi, J. Stanojevic, A. Ourjoumtsev, P. Grangier, Homodyne tomography of a single photon retrieved on demand from a cavity-enhanced cold atom memory. Phys. Rev. Lett. **112**, 033601 (2014).

[26] H. Li, J.-P. Dou, X.-L. Pang, T.-H. Yang, C.-N. Zhang, Y. Chen, J.-M. Li, I. A. Walmsley, X.-M. Jin, Heralding quantum entanglement between two room-temperature atomic ensembles. Optica **8**, 925-929 (2021).

[27] K. B. Dideriksen, R. Schmieg, M. Zugenmaier, E. S. Polzik, Room-temperature single-photon source with near-millisecond built-in memory. Nat. Commun. **12**, 3699 (2021).

[28] C. Laplane, P. Jobez, J. Etesse, N. Gisin, M. Afzelius, Multimode and Long-Lived Quantum Correlations Between Photons and Spins in a Crystal. Phys. Rev. Lett. **118**, 210501 (2017).

[29] K. Kutluer, M. Mazzera, H. de Riedmatten, Solid-State Source of Nonclassical Photon Pairs with Embedded Multimode Quantum Memory. Phys. Rev. Lett. **118**, 210502 (2017).

[30] S. -J. Yang, X. -J. Wang, J. Li, J. Rui, X. -H. Bao, J. -W. Pan, Highly retrievable spin-wave-photon entanglement source. Phys. Rev. Lett. **114**, 210501 (2015).

[31] Y. Yu, F. Ma, X. -Y. Luo, B. Jing, P. -F. Sun, R. -Z. Fang, C. -W. Yang, H. Liu, M. -Y. Zheng, X. -P. Xie, W. -J. Zhang, L. -X. You, Z. Wang, T. -Y. Chen, Q. Zhang, X. -H. Bao, J. -W. Pan, Entanglement of two quantum memories via fibers over dozens of kilometers. Nature **578**, 240-245 (2020).

[32] Y. O. Dudin, A. G. Radnaev, R. Zhao, J. Z. Blumoff, T. A. Kennedy, A. Kuzmich, Entanglement of light-shift compensated atomic spin waves with telecom light. Phys. Rev. Lett. **105**, 260502 (2010).

[33] X. -J. Wang, S. -J. Yang, P. -F. Sun, B. Jing, J. Li, M. -T. Zhou, X. -H. Bao, J. -W. Pan, Cavity-Enhanced Atom-Photon Entanglement with Sub-second Lifetime. Phys. Rev. Lett. **126**, 090501 (2021).

[34] S.-Z. Wang, M.-J. Wang, Y.-F. Wen, Z.-X. Xu, T.-F. Ma, S.-J. Li, H. Wang, Long-lived and multiplexed atom-photon entanglement interface with feed-forward-controlled readouts. Communications Physics **4**, 168 (2021).

[35] R. Ikuta, T. Kobayashi, T. Kawakami, S. Miki, M. Yabuno, T. Yamashita, H. Terai, M. Koashi, T. Mukai, T. Yamamoto, and N. Imoto,

Polarization insensitive frequency conversion for an atom-photon entanglement distribution via a telecom network. Nat. Commun. **9**, 1997 (2018).

[36] Y. -F. Pu, N. Jiang, W. Chang, H. -X. Yang, C. Li, L. -M. Duan, Experimental realization of a multiplexed quantum memory with 225 individually accessible memory cells. Nat. Commun. **8**, 15359 (2017).

[37] Y.-F. Pu, S. Zhang, Y.-K. Wu, N. Jiang, W. Chang, C. Li, L.-M. Duan, Experimental demonstration of memory-enhanced scaling for entanglement connection of quantum repeater segments. Nat. Photon. **15**, 374-378 (2021).

[38] H. Tanji, S. Ghosh, J. Simon, B. Bloom, and V. Vuletic, Heralded Single-Magnon Quantum Memory for Photon Polarization States, Phys. Rev. Lett. **103**, 043601 (2009).

[39] C. Liu, Z. Dutton, C. H. Behroozi and L. V. Hau, Observation of coherent optical information storage in an atomic medium using halted light pulses. Nature **409** 490 (2001).

[40] D. Phillips, A. Fleischhauer, A. Mair, R. Walsworth and M. D. Lukin, Storage of Light in Atomic Vapor. Phys. Rev. Lett. **86** 783 (2001).

[41] M. D. Eisaman, A. Andre, F. Massou, M. Fleischhauer, A. S. Zibrov, and M. D. Lukin, Electromagnetically induced transparency with tunable single-photon pulses. Nature **438**, 837 (2005).

[42] T. Chaneliere, D. N. Matsukevich, S. D. Jenkins, S. Y. Lan, T. A.

Kennedy, and A. Kuzmich, Storage and retrieval of single photons transmitted between remote quantum memories. Nature **438**, 833 (2005).

[43] K. S. Choi, H. Deng, J. Laurat and H. J. Kimble, Mapping photonic entanglement into and out of a quantum memory. Nature **452**, 67–71 (2008).

[44] Z.-X. Xu, Y.-L. Wu, L. Tian, L.-R. Chen, Z.-Y. Zhang, Z.-H. Yan, S.-J. Li, H. Wang, C.-D. Xie, K.-C. Peng, Long lifetime and high-fidelity quantum memory of photonic polarization qubit by lifting Zeeman degeneracy. Phys. Rev. Lett. **111**, 240503 (2013).

[45] S.-Y. Zhou, S.-C. Zhang, C. Liu, J. -F. Chen, J.-M. Wen, M. M. T. Loy, G. K. L. Wong, S.-W. Du, Optimal storage and retrieval of single-photon waveforms. Optics express **20**, 24124 (2012).

[46] G. Heinze, C. Hubrich, T. Halfmann, Stopped light and image storage by electromagnetically induced transparency up to the regime of one minute. Phys. Rev. Lett. **111**, 033601 (2013).

[47] Y. -H. Chen, M. J. Lee, I. -C. Wang, S.-W Du, Y. -F. Chen, Y. -C. Chen, I. A. Yu, Coherent optical memory with high storage efficiency and large fractional delay. Phys. Rev. Lett. **110**, 083601 (2013).

[48] Y. F. Hsiao, P. J. Tsai, H. -S. Chen, S. -X. Lin, C. -C. Hung, C. -H. Lee, Y. -H. Chen, Y. -F. Chen, I. A. Yu, Y. -C. Chen, Highly Efficient Coherent Optical Memory Based on Electromagnetically Induced Transparency. Phys. Rev. Lett. **120**, 183602 (2018).

[49] P. Vernaz-Gris, K. Huang, M.-T. Cao, A. S. Sheremet, J. Laurat,

Highly-efficient quantum memory for polarization qubits in a spatially-multiplexed cold atomic ensemble. Nat. Commun. **9**, 363 (2018).

[50] Y.-F. Wang, J.-F. Li, S.-C. Zhang, K.-Y Su, Y.-R. Zhou, K.-Y. Liao, S.-W. Du, H. Yan, S.-L. Zhu, Efficient quantum memory for single-photon polarization qubits. Nat. Photon. **13**, 346-351 (2019).

[51] M. Cao, F. Hoffet, S. Qiu, A. S. Sheremet, and J. Laurat, Efficient reversible entanglement transfer between light and quantum memories, Optica **7 ,**1440-1444(2020)

[52] Z. Yan, L. Wu, X. Jia, Y. Liu, R. Deng, S. Li, H. Wang, C. Xie, and K. Peng, Establishing and storing of deterministic quantum entanglement among three distant atomic ensembles. Nat. Commun. **8**, 718 (2017).

[53] E. Saglamyurek, N. Sinclair, J. Jin, J. A. Slater, D. Oblak, F. Bussieres, M. George, R. Ricken, W. Sohler, W. Tittel, Broadband waveguide quantum memory for entangled photons. Nature **469**, 512-515 (2011).

[54] C. Clausen, I. Usmani, F. Bussieres, N. Sangouard, M. Afzelius, H. de Riedmatten, N. Gisin, Quantum storage of photonic entanglement in a crystal. Nature **469**, 508-511 (2011).

[55] E. Saglamyurek, J. Jin, V. B. Verma, M. D. Shaw, F. Marsili, S. W. Nam, D. Oblak, and W. Tittel, Quantum storage of entangled telecom-wavelength photons in an erbium-doped optical fibre. Nat. Photon. **9**, 83 (2015).

[56] K. R. Ferguson, S. E. Beavan, J. J. Longdell, and M. J. Sellars,

Generation of Light with Multimode Time-Delayed Entanglement Using Storage in a Solid-State Spin-Wave Quantum Memory. Phys. Rev. Lett. **117**, 020501 (2016).

[57] Y. -W. Cho, G. T. Campbell, J. L. Everett, J. Bernu, D. B. Higginbottom, M. -T. Cao, J. Geng, N. P. Robins, P. K. Lam, B. C. Buchler, Highly efficient optical quantum memory with long coherence time in cold atoms. Optica **3**, 100-107 (2016).

[58] M. Sabooni, Q. Li, S. Kroll, L. Rippe, Efficient quantum memory using a weakly absorbing sample. Phys. Rev. Lett. **110**, 133604 (2013).

[59] N. Sinclair, E. Saglamyurek, H. Mallahzadeh, J. A. Slater, M. George, R. Ricken, M. P. Hedges, D. Oblak, C. Simon, W. Sohler, W. Tittel, Spectral multiplexing for scalable quantum photonics using an atomic frequency comb quantum memory and feed-forward control. Phys. Rev. Lett. **113**, 053603 (2014).

[60] M. Hosseini, G. Campbell, B. M. Sparkes, P. K. Lam, and B. C. Buchler, Unconditional Room Temperature Quantum Memory. Nat. Phys. **7**, 794 (2011).

[61] K. F. Reim, J. Nunn, V. O. Lorenz, B. J. Sussman, K. C. Lee, N. K. Langford, D. Jaksch, and I. A. Walmsley, Towards high-speed optical quantum memories. Nat. Photon. **4**, 218 (2010).

[62] J. Guo, X. Feng, P. Yang, Z. Yu, L. Q. Chen, C. H. Yuan, and W. Zhang, High-performance Raman quantum memory with optimal control in room

temperature atoms. Nat. Commun. **10**, 148 (2019).

[63] D.-S. Ding, W. Zhang, Z.-Y. Zhou, S. Shi, B.-S. Shi, G.-C. Guo, Raman quantum memory of photonic polarized entanglement. Nat. Photon. **9**, 332-338 (2015).

[64] K. T. Kaczmarek, P. M. Ledingham, B. Brecht, S. E. Thomas, G. S. Thekkadath, O. Lazo-Arjona, J. H. D. Munns, E. Poem, A. Feizpour, D. J. Saunders, J. Nunn, I. A. Walmsley, High-speed noise-free optical quantum memory. Phys. Rev. A **97**, 042316 (2018).

[65] Ran Finkelstein, Eilon Poem, Ohad Michel, Ohr Lahad, O. Firstenberg, Fast, noise-free memory for photon synchronization at room temperature. Sci. Adv. **4**, eaap8598 (2018).

[66] C. Simon, H. de Riedmatten, M. Afzelius, N. Sangouard, H. Zbinden, N. Gisin, Quantum repeaters with photon pair sources and multimode memories. Phys. Rev. Lett. **98**, 190503 (2007).

[67]. England, D. G. et al. High-fidelity polarization storage in a gigahertz bandwidth quantum memory. J. Phys. B- Mol. Opt. **45**, 124008 (2012).

[68]. Cho, Y.-W. and Kim, Y.-H. Atomic vapor quantum memory for a photonic polarization qubit. Opt. Express **18**, 25786–25793 (2010).

[69] K. C. Cox, D. H. Meyer, Z. A. Castillo, F. K. Fatemi, P. D. Kunz, Spin-Wave Multiplexed Atom-Cavity Electrodynamics. Phys. Rev. Lett. **123**, 263601 (2019).

[70] L. Heller, P. Farrera, G. Heinze, and H. de Riedmatten, Cold-Atom

Temporally Multiplexed Quantum Memory with Cavity-Enhanced Noise Suppression. Phys. Rev. Lett. **124**, 210504 (2020).

[71] See Supplemental Material

Supplementary Files

This is a list of supplementary files associated with this preprint. Click to download.

- Supplementarymaterial10.docx